HHS Public Access

Author manuscript

Br J Haematol. Author manuscript; available in PMC 2015 April 09.

Published in final edited form as:

Br J Haematol. 2011 December ; 155(5): 588–598. doi:10.1111/j.1365-2141.2011.08888.x.

Preclinical Evaluation of a Novel SIRT1 Modulator SRT1720 in Multiple Myeloma Cells

Dharminder Chauhan[¶,*], **Madhavi Bandi**[*], **Ajita V. Singh**, **Arghya Ray**, **Noopur Raje**, **Paul Richardson**, and **Kenneth C. Anderson**

The LeBow Institute for Myeloma Therapeutics and Jerome Lipper Myeloma Center, Department of Medical Oncology, Dana Farber Cancer Institute, Harvard Medical School, Boston, MA

Summary

SIRT1 belongs to the silent information regulator 2 (Sir2) protein family of enzymes and functions as a NAD^+-dependent class III histone deacetylase. Here, we examined the anti-multiple myeloma (MM) activity of a novel oral agent, SRT1720, which targets SIRT1. Treatment of MM cells with SRT1720 inhibited growth and induced apoptosis in MM cells resistant to conventional and bortezomib therapies without significantly affecting the viability of normal cells. Mechanistic studies showed that anti-MM activity of SRT1720 is associated with: 1) activation of caspase-8, caspase-9, caspase-3, poly (ADP) ribose polymerase; 2) increase in reactive oxygen species; 2) induction of phosphorylated ataxia telangiectasia mutated/checkpoint kinase 2 signalling; 3) decrease in vascular endothelial growth factor-induced migration of MM cells and associated angiogenesis; and 4) inhibition of nuclear factor-κB. Blockade of ATM attenuated SRT1720-induced MM cell death. In animal tumour model studies, SRT1720 inhibited MM tumour growth. Finally, SRT1720 enhanced the cytotoxic activity of bortezomib or dexamethasone. Our preclinical studies provide the rationale for novel therapeutics targeting SIRT1 in MM.

Keywords

Multiple Myeloma; Apoptosis; Microenvironment

Introduction

Recent studies have provided evidence for the potential clinical utility of targeting histone deacetylase (HDAC) enzymes in multiple myeloma (MM) (Catley *et al*, 2006; Hideshima *et al*, 2005), and other haematological malignancies (Bhalla *et al*, 2009; Dai *et al*, 2008; Dasmahapatra *et al* 2010; Grant *et al*, 2007). The sirtuins (SIRTs), also known as silent information regulator-2 (Sir2) proteins, consists of nicotinamide adenine dinucleotide

[¶]Address correspondence: Kenneth C. Anderson and Dharminder Chauhan, Dana-Farber Cancer Institute, Mayer Building Room 561, 44 Binney Street, Boston, MA 02115, Tel:617-632-4563, Fax:617-632-2140, Kenneth_Anderson@dfci.harvard.edu, Dharminder_Chauhan@dfci.harvard.edu.

[*]Contributed equally to the work

Authors' contributions: D.C. designed research, analysed data, and wrote the manuscript; M.B. performed most of the experiments and interpreted data; A.V.S., helped in xenograft studies; AR helped in cell viability assays; N.R. and P.R. provided clinical samples; and K.C.A. analysed data and wrote the manuscript.

Conflict-of-interest disclosure: None of the authors have competing financial interests

(NAD)-dependent deacetylases (class III) that are involved in various cellular processes from aging to cancer (Dai *et al*, 2010; Haigis and Sinclair 2010; Milne and Denu 2008; Sauve, 2009). While many HDACs have been extensively studied, the role of SIRTs in MM remains undefined.

SIRTs are distinct from the "classical" class I/II/IV HDACs because they do not have any sequence similarity with other HDACs and are not sensitive to HDAC inhibitors (Borra *et al*, 2002; Imai *et al*, 2000; Jackson & Denu 2002). Furthermore, SIRTs act *via* NAD^+-dependent deacetylation, whereas HDACs utilize Zn^{2+}-dependent deacetylation. To date, seven human sirtuins (SIRT1-SIRT7) have been identified; among these, SIRT1 is the closest homologue of yeast Sir2 and modulates p53, nuclear factor (NF)-κB, peroxisome proliferator-activated receptor-γ coactivator (PGC)-1α, liver X receptor (LXR) and Fork head transcription factors (Sauve, 2009). SIRT1 modifies both histones (histone H1, histone H3 and histone H4) and non-histone proteins that are involved in apoptosis, cell growth, metabolism, caloric restriction and cell senescence (Dai *et al*, 2010; Haigis & Sinclair 2010; Sauve 2009).

Prior *in vitro* and *in vivo* studies using various cancer cell models show a role of *SIRT1* either as an oncogene or a tumour suppressor gene. The oncogenic potential of SIRT1 is exemplified by studies showing that blockade of SIRT1, like other HDACs, triggers growth arrest and apoptosis in breast, colon and lung cancers (Ford *et al*, 2005; Heltweg *et al*, 2006; Ota *et al*, 2006). In contrast, the tumour suppressor function of SIRT1 is evident from several *in vivo* and *in vitro* studies showing that SIRT1 is proapoptotic and anti-proliferative (Chua *et al*, 2005; Firestein *et al*, 2008; Fu *et al*, 2006; Wang *et al*, 2008; Yeung *et al*, 2004). For example, mouse embryonic fibroblastsobtained from SIRT1-null mice are susceptible to spontaneous immortalization, implicating a growth-suppressive function of SIRT1 (Chua *et al*, 2005). Haematopoietic stem cells from SIRT1-null mice exhibit enhanced proliferation ability, and shRNA knockdown of *SIRT1* in human fibroblasts accelerates cell proliferation (Abdelmohsen *et al*, 2007; Narala *et al*, 2008). Another study showed that SIRT1 blocks androgen receptor-dependent growth in prostrate cancer cells (Fu *et al*, 2006). Biochemical inhibition of SIRT1 with specific inhibitors has not been shown to prevent proliferation of multiple cancer cell lines (Kamel *et al*, 2006; Solomon *et al*, 2006; Stunkel *et al*, 2007). Ectopic expression of SIRT1 led to reduced proliferation in colon cancer cell lines and attenuated tumour growth in animal models (Kabra *et al*, 2009); and conversely, SIRT1-deficiency resulted in an increased tumour formation in p53-null mice (Wang *et al*, 2008). Finally, SIRT1 was found to inhibit β-catenin, a member of Wnt signalling pathway, resulting in suppression of intestinal tumourigenesis and colon cancer growth (Firestein *et al*, 2008). These studies support the potential of SIRT1 as tumour suppressor, and provide the rationale for preclinical evaluation of activators of SIRT1 in the treatment of cancer.

Recent medical chemistry research, using high-throughput screening and mass spectrometry, identified small molecule activators of SIRT1 that are both potent and selective (Milne & Denu, 2008). In the present study, we examined the efficacy of one such novel first-in-class SIRT1 activator SRT1720 in MM using *in vitro* and *in vivo* models.

Materials and Methods

Cell culture

MM cell lines including MM.1S (dexamethasone-sensitive), MM.1R (dexamethasone-resistant), RPMI-8226, LR-5 (melphalan-resistant derivative of RPMI-8226), U266, KMS12, and INA-6 (interleukin-6 dependent) were cultured with RPMI-1640 medium supplemented with 10% fetal bovine serum (FBS), 2mM L-glutamine, 100 units/ml Pencillin and 100 ug/ml streptomycin. Tumour cells from MM patients were purified (greater than 95% purity) by CD138 positive selection using the Auto MACS magnetic cell sorter (Miltenyi Biotec Inc., Auburn, CA). Informed consent was obtained from all patients in accordance with the Helsinki protocol. Peripheral blood mononuclear cells (PBMCs) from healthy donors were maintained in culture medium, as above. PBMCs were also labelled with CD19 microbeads for direct magnetic isolation of B-cells by positive selection using Auto MACS magnetic cell sorter (Miltenyi Biotec Inc.). The magnetically sorted CD19-positive cells were further stained with human CD20-fluoescein isothiocycante (FITC) antibody (Miltenyi Biotec Inc.) and analysed by flow cytometry. SRT1720 was obtained from Sirtris (Cambridge, MA); bortezomib was purchased from Selleck Chemicals LLC (Houston, TX); and dexamethasone was obtained from Calbiochem (San Deigo, CA).

Fluor de Lys Deacetylase Assay

Deacetylase activity of SIRT1 was measured using the *Fluor de Lys* Deacetylase kit (BIOMOL international Inc, Plymouth Meeting, PA) according to the manufacturer's instructions. Briefly, 4×10^4 cells were plated in 50 μl of medium containing 200 μM flour-de lys substrate; the plate was then incubated for 5 h at 37°C, followed by addition of 100 μl of 2 μM Trichostatin A developing solution. After further incubation for 15 min at 37°C, the fluorescence was measured using SpectraMax M5 Multi-Mode Microplate Readers (Molecular Devices, Inc., Sunnyvale, CA).

Cell viability and apoptosis assays

Cell viability was assessed with a colorimetric assay using 3-(4, 5-dimethylthiozol-2-yl)-2, 5-diphenyltetrazolium bromide (MTT; Calbiochem) as described previously (Hideshima *et al*, 2000). Apoptosis assay was quantified using Annexin V-FITC/Propidium iodide (PI) apoptosis detection kit, as per manufacturer's instructions (BD Biosciences, San Jose, CA), followed by analysis on FACS Calibur (BD Biosciences).

Western blotting and protein quantification

Immunoblot analysis was performed using antibodies against caspase-3, caspase-7, caspase-8, caspase-9, poly (ADP) ribose polymerase (PARP) (Cell Signaling, Beverly, MA), Ace-Lys 382 p53, phosphorylated-ataxia telangiectasia mutated (pATM), phosphorylated-checkpoint kinase 2 (pCHK2), phosphorylated-IκB ser32/36, and GAPDH (Abcam, Cambridge, MA). Blots were then developed by enhanced chemiluminescence (ECL; Amersham, Arlington Heights, IL). Densitometry of protein bands was acquired using an AlphaImager EC gel documentation system (Alpha Innotec, Kasendorf, Germany), and

bands were analysed using the spot densitometry analysis tool (Alpha Ease FC software, version, 4.1.0).

Human plasmacytoma xenograft model

All animal studies were approved by the Institutional Animal Care and Use Committee of the Dana Farber Cancer Institute. The xenograft tumour model was performed as previously described (LeBlanc *et al*, 2002). This animal model has been immensely useful in extensively validating the novel anti-MM therapies, bortezomib and lenalidomide, leading to their translation to clinical trials and US Food and Drug Administration approval for the treatment of MM. Fox Chase-SCID mice (6 mice each group) were subcutaneously inoculated with 6.0×10^6 MM.1S cells in 100 μl of serum-free RPMI-1640 medium. When tumours were measurable (~100 mm^3) approximately three weeks after MM cell injection, mice were treated orally with vehicle alone (20% PEG400/0.5% Tween80/79.5% deionized water) or SRT1720 (200 mg/kg) for four weeks on a five consecutive days/week schedule.

In situ detection of apoptosis using immunohisto-chemistry (IHC)

Tumours from vehicle (control)- and SRT1720-treated mice were excised and preserved in 10% formalin. Apoptotic cells in tumours were identified by IHC staining for caspase-3 activation, as previously described (Chauhan *et al*, 2010).

In vitro migration and capillary-like tube structure formation assays

Transwell Insert Assays (Chemicon, Billerica, MA) were utilized to measure migration as previously described (Podar *et al*, 2001). *In vitro* angiogenesis was assessed by Matrigel capillary-like tube structure formation assay (Chauhan *et al*, 2010). For endothelial tube formation assay, human vascular endothelial cells (HUVECs) were obtained from Clonetics (Walkersville, MD) and maintained in endothelial cell growth medium-2 (EGM2 MV SingleQuots, Clonetics) containing 5% FBS. After three passages, HUVEC cell viability was measured with the trypan blue exclusion assay, and <5% of cell death was observed with SRT1720 treatment.

Statistical Analysis

Statistical significance of differences observed in drug-treated *vs.* control cultures was determined by the Student's *t* test. The minimal level of significance was $P < 0.05$. Tumour volume in mice was measured using the GraphPad PRISM (GraphPad Software, SanDiego, CA).

Results

SRT-1720 targets SIRT1

We confirmed the functional specificity of SRT1720 against SIRT1 using different experimental strategies. For these studies, we first utilized the *Fluor de Lys* Deacetylase assay to measure whether SRT1720 affects SIRT1 deacetylase enzymatic activity. Treatment of MM.1R and RPMI-8226 MM cells with SRT1720 markedly increased the deacetylating activity; conversely, pre-treatment of cells with nicotinamide, an inhibitor of

SIRT1, significantly blocked SRT1720-triggered deacetylating activity (Fig 1A). Secondly, immunoblot analysis using antibodies specific against acetylated p53 (a known substrate of SIRT1) showed a marked decrease in acetylated state of p53 in SRT1720-treated MM cells (Fig 1B). Our data is in agreement with previous reports showing that SRT1720-induced biological effects occur *via* SIRT1 (Bhardwaj *et al*, 2007; Funk *et al*, 2010; Yoshizaki *et al*, 2009).

Anti-MM activity of SRT1720

Human MM cell lines (MM.1S, MM.1R, RPMI-8266, LR-5, INA6, KMS12, U266) were treated with various concentrations of SRT1720 for 24 h, followed by assessment for cell viability using MTT assays. A significant concentration-dependent decrease in viability of all cell lines was noted in response to treatment with SRT1720 (Fig 1C; $P < 0.005$ for all cell lines; n=3). To determine whether SRT1720 similarly affects purified patient cells, tumour cells from six MM patients relapsing after multiple prior therapies including dexamethasone, melphalan, bortezomib, or lenalidomide and were treated for 24 h with SRT1720, followed by assessment for cell viability. A significant decrease in cell viability of all patient tumour cells was noted after SRT1720 treatment (Fig 1D; IC_{50} range: 3–5 μM; $P < 0.005$ for all patients). Patients were considered refractory to specific therapy when disease progressed on therapy or relapsed within two months of stopping therapy. Similar to our data using drug resistant cell lines, we found responses in patient-derived tumour cells, including those resistant to therapies such as bortezomib, dexamethasone, or lenalidomide. A similar response to SRT1720 treatment was noted in two untreated patient MM cells (data not shown). Importantly, the 50% inhibitory concentration (IC_{50}) for MM cells of SRT1720 is at concentrations that do not significantly affect viability of normal lymphocytes (Fig 1E; n =2). Higher concentrations of SRT1720 (15 μM) induced a modest (10–20%) decrease in normal cell viability. Additionally, treatment of B cells obtained from normal healthy donors with SRT1720 showed no marked decrease in the viability of these cells (Fig 1F). Together, our data demonstrate that SRT1720 triggers cytotoxicity in MM cells, without significant toxicity in normal PBMCs.

We next examined whether the SRT1720-triggered decrease in viability was due to apoptosis. SRT1720 induced a significant increase in the Annexin V^+/PI^- apoptotic cell population in RPMI-8226 and MM.1R cells (Fig 1G; $P < 0.04$, n=3). Moreover, treatment of both MM.1R and RPMI-8226 cells with SRT1720 triggered a marked increase in proteolytic cleavage of PARP (Lazebnik *et al*, 1994), a signature event during apoptosis (Fig 1H and 1I).

Mechanisms mediating anti-MM activity of SRT1720

Mitochondria mediate apoptotic signalling *via* activation of the cell death initiator caspase, pro-caspase 9 (intrinsic apoptotic pathway) (Bossy-Wetzel & Green 1999). Similarly, Fas associated death-domain (FADD) protein is an essential part of the death-inducing signalling complexes (DISCs) that assemble upon engagement of tumour necrosis factor receptor family members, such as Fas, resulting in proteolytic processing and autoactivation of pro-caspase-8 (extrinsic apoptotic pathway)(Strasser *et al*, 2000). Our data show that SRT1720 induced activation of both casapse-8 and caspase-9 apoptotic pathways (Fig 2A). Both

caspase-9 and caspase-8 are known to activate a common downstream effector procapsase-3 (Miller, 1999), and our data further showed that SRT1720 triggered caspase-3 activation, as evidenced by caspase-3 cleavage (Fig 2A). Moreover, SRT1720-induced apoptosis in MM cells was associated with generation of reactive oxygen species (ROS)(Fig 2B and 2C), suggesting disruption of mitochondrial integrity (Miller, 1999). Together, these findings suggest that SRT1720-induced apoptosis in MM cells occurs *via* both mitochondria-independent and mitochondria-dependent apoptotic signalling pathways.

SIRT1 plays an important role in DNA damage response and DNA repair activity (Chen *et al*, 2009; Wang *et al*, 2008). The DNA damage response is, in part, mediated via activation of ATM, a serine/threonine protein kinase that is recruited and activated by DNA double-strand breaks. ATM phosphorylates several key proteins that activate DNA damage checkpoint, thereby triggering cell cycle arrest, DNA repair or apoptosis (Yuan & Seto 2007). Given that SIRT1 is linked to DNA damage response (Chen *et al*, 2009; Wang *et al*, 2008), and SRT1720 targets SIRT1 (Funk *et al*, 2010; Yoshizaki *et al*, 2009), we next examined whether SRT1720 triggers the ATM-mediated apoptotic signalling pathway. Treatment of RPMI-8226 and MM.1R cells with SRT1720 induced phosphorylation of ATM (pATM) (Fig 3A). We further confirmed these data by quantification of pATM using an enzyme-linked immunosorbent assay (ELISA): SRT1720 triggered a significant (3- to 4-fold) increase in pATM levels in MM.1R and RPMI-8226 cells (Fig 3B). Examination of CHK2, a known downstream target of ATM, showed a marked increase in phosphorylation in response to SRT1720 (Fig 3C), suggesting that SRT1720-induced MM cell apoptosis occurs *via* activation of the ATM-CHK2 signalling axis. Importantly, blockade of ATM using a biochemical inhibitor KU5593 abrogated SRT1720-induced decrease in cell viability (Fig 3D). KU-55933 alone did not affect the viability of MM cells (data not shown). Taken together, these data suggest that the anti-MM activity of SRT1720 predominantly relies on the ATM-CHK2/caspase 8/9 signalling axis.

Besides activation of pro-apoptotic signalling cascades, we also examined whether SRT1720 affects growth and survival signalling pathways. Among many, the NF-κB-mediated signalling cascade has been shown to play a role in growth, survival, and drug resistance in MM cells (Chauhan *et al*, 1996; Hideshima *et al*, 2002). Specifically, adhesion of MM cells to bone marrow stromal cells triggers NF-κB- mediated transcription and secretion of various MM cell growth factors (Chauhan *et al*, 1996). In the present study, treatment of MM cells with SRT1720 significantly blocked NF-κB activity, evidenced by a decrease in IκB-α activity (Fig 3E; a 90% decrease in IκB-α activity was noted in SRT1720 *vs.* untreated cells). These findings suggest that the inhibition of NF-κB activity contributes to the overall anti-MM activity of SRT1720.

SRT1720 blocks migration of MM cells and angiogenesis

We and others have shown that migration and angiogenesis play an important role in the progression of MM (Podar *et al*, 2001; Vacca *et al*, 1999). We investigated whether SRT1720 has anti-angiogenic activity. The effect of SRT1720 on these events was therefore examined using Transwell insert systems and *in vitro* tubule formation assays. Serum alone markedly increased MM.1S cell migration; importantly, SRT1720 significantly inhibited

serum-dependent MM.1S cell migration, as evidenced by a decrease in the number of crystal violet-stained cells (Fig 4A). Vascular endothelial growth factor (VEGF) is elevated in the MM bone marrow microenvironment, and triggers growth, migration, and angiogenesis in MM (Kumar *et al*, 2003; Podar *et al*, 2001; Podar *et al*, 2002; Rajkumar & Witzig 2000; Vacca *et al*, 1999). We next examined whether SRT1720 affects VEGF-induced MM cell migration. VEGF alone markedly increased MM.1S cell migration; conversely, SRT1720 significantly ($P = 0.04$, n=3) inhibited VEGF-dependent MM cell migration (Fig 4B). Cells remained >95% viable before and after performing the migration assay, excluding the possibility that drug-induced inhibition of migration was due to cell death.

We next utilized *in vitro* capillary-like tube structure formation assays to assess whether SRT1720 induces anti-angiogenic effects. Angiogenesis was measured *in vitro* using Matrigel capillary-like tube structure formation assays: HUVECs plated onto Matrigel differentiate and form capillary-like tube structures similar to *in vivo* neovascularization, a process dependent on cell-matrix interaction, cellular communication, and cellular motility. This assay provides evidence for anti-angiogenic effects of drugs. HUVECs were seeded in 96-well culture plates precoated with Matrigel; treated with vehicle (dimethyl sulphoxide, DMSO) or SRT1720 for 12 h; and then examined for tube formation using an inverted microscope. Tubule formation was markedly decreased in a dose-dependent manner in SRT1720-treated cells, but not in DMSO control cells (Fig 4C and 4D). HUVEC cell viability was assessed using Trypan blue exclusion assay: < 5% cell death was observed after SRT1720 treatment, excluding the possibility that drug-induced inhibition of capillary-tube formation was due to cell death. These findings suggest that SRT1720 blocks migration and angiogenesis.

SRT1720 inhibits human MM cell growth *in vivo*

Having shown that SRT1720 induced apoptosis in MM cells *in vitro*, we next examined the *in vivo* efficacy of SRT1720 treatment using a the human plasmacytoma MM.1S xenograft mouse model (Chauhan *et al*, 2008; LeBlanc *et al*, 2002). A significant reduction (P=0.008) in tumour growth was observed in mice receiving SRT1720 treatment relative to untreated mice (Fig 5A). Examination of the xenografted tumour sections showed that SRT1720, but not vehicle alone, increased the number of cleaved-caspase-3 positive cells (Fig 5B, left panels). Furthermore, a significant decrease in proliferation marker Ki-67-positive cells was also noted in tumour sections from SRT1720-treated mice relative to control mice (Fig 5B, right panels). In agreement with previously reported findings using SIRT1 activating agents (Funk *et al*, 2010; Yoshizaki *et al*, 2009), we found no toxicity in the MM xenograft model even upon treatment of mice with SRT1720 at 200 mg/kg doses. These data demonstrate potent anti-tumour activity of SRT1720 *in vivo*.

Combination of SRT1720 with bortezomib, or dexamethasone triggers additive anti-MM activity

Human MM cell lines (MM.1S, RPMI-8226, and MM.1R) were treated with SRT1720 and bortezomib or dexamethasone for 24 h, followed by assessment for cell viability using MTT assays. For these studies, we utilized SRT1720, bortezomib, or dexamethasone at concentrations lower than their maximal cytotoxic concentration for each cell line. A more

significant decrease in viability of all cell lines was observed in response to treatment with SRT1720 combined with low doses of bortezomib or dexamethasone (Fig 6A–6D; n = 3) than with either agent alone. For example, treatment of MM.1S cells with low doses of SRT1720 (5 μM) and bortezomib (3 nM) triggered 60% decrease in viability, whereas only minimal cell killing was observed using either of these agents alone at these low concentrations (Fig 6A). These data suggests that SRT1720 enhances the anti-MM activity of bortezomib or dexamethasone.

Discussion

Previous reports have demonstrated the anti-tumour activity of a SIRT1 activator (Bhardwaj *et al*, 2007; Harper *et al*, 2007; Sexton *et al*, 2006). Mass-spectrometry based assays identified SRT1720 as a more potent, and selective small molecule activator of SIRT1 (Milne & Denu, 2008). In the context of SRT1720-mediated biological effects, it is known that SRT1720 interacts directly with SIRT1 and triggers SIRT1-catalysed deacetylation *via* an allosteric mechanism (Dai *et al*, 2010). Activation of SIRT1 by SIRT1 activating compounds is dependent on structural features of the substrate (Dai *et al*, 2010; Milne & Denu 2008; Pacholec *et al*, 2010). Our data showed that SRT1720 markedly increases the SIRT1 deacetylating enzymatic activity in MM cells; conversely, pre-treatment of cells with nicotinamide (an inhibitor of SIRT1) blocked SRT1720-triggered activity. These findings are in agreement with prior biochemical and cell-based studies (Dai *et al*, 2010; Milne & Denu 2008), suggesting that SIRT1 is a target of SRT1720.

Examination of SRT1720-induced biological sequelae in MM cells showed that SRT1720 decreases the viability of MM cell lines and primary patient tumour cells, without affecting normal PBMCs viability. Importantly, our data demonstrate anti-MM activity of SRT1720 in MM cell lines, including those sensitive and resistant to therapies, as well as representing distinct cytogenetic profiles. For example, we evaluated the isogenic cell lines, MM.1S (dexamethasone-sensitive) and MM.1R (dexamethasone-resistant), with t(14;16) translocation and *MAF* overexpression; RPMI-8266 with *TP53*, *KRAS* and *EGFR* mutations; INA-6, an interleukin-6-dependent cell line with *NRAS* activating mutation, and KMS12 t(11:14) with *CCND1* deregulation (Avet-Loiseau *et al*, 2007; Bergsagel & Kuehl 2005; Burger *et al*, 2001; Davies *et al*, 2003; Greenstein *et al*, 2003; Hideshima *et al*, 2007). The observed variation in IC_{50} of SRT1720 for each cell line may be due to the heterogeneous nature of MM and drug resistance (Bergsagel *et al*, 1996; Bergsagel & Kuehl 2005; Davies *et al*, 2003; Hideshima *et al*, 2007). In addition, the ATM abnormalities and/or p53 status in MM cells may contribute to SRT1720 anti-MM activity, and this issue remains to be defined. Nonetheless, our present findings showed similar responses in patient-derived tumour cells, including those resistant to therapies such as bortezomib, dexamethasone, or lenalidomide.

Mechanistic studies showed that anti-MM activity of SRT1720 is associated with activation of the caspase cascade, ROS generation, and apoptotic signalling involving the ATM/CHK2 pathway. Blockade of ATM abrogated SRT1720-induced MM cell death. Although ATM-CHK2 signalling plays a key role in mediating apoptosis triggered by SRT1720, the possibility that other signaling pathways are also activated by SRT1720 cannot be excluded.

Overall, our current study suggests that the anti-MM activity of SRT1720 involves the ATM-CHK2/caspase 8/9 signalling axis.

In addition to inducing an apoptotic signalling cascade, SRT1720 also blocks one of the major growth and survival signalling cascades occurring *via* NF-κB. These findings demonstrate the ability of SRT1720 to simultaneously trigger apoptotic signalling, as well as block growth and survival pathways in MM cells. Our ongoing studies are focused on further delineating the mechanism of action of SRT1720 either alone or together with other agents.

Besides *in vitro* studies, we also examined anti-MM activity of SRT1720 *in vivo*. A marked growth inhibitory effect of SRT1720 was observed in a human plasmacytoma xenograft mouse model. In agreement with other *in vivo* animal model studies (Bhardwaj *et al*, 2007; Funk *et al*, 2010; Yoshizaki *et al*, 2009) using SIRT1-activating agents, no toxicity was observed during treatment of mice with SRT1720 at 200 mg/kg doses. The remarkable anti-MM activity of SRT1720 *in vivo* was confirmed by IHC analysis of tumours harvested from control and SRT1720-treated mice using molecular markers of apoptosis and proliferation (caspase-3 and Ki-67, respectively). The *in vivo* findings confirmed our *in vitro* data suggesting the potent anti-MM activity of SRT1720. Finally, we also examined the effect of SRT1720 in combination with a proteasome inhibitor, bortezomib, and a conventional anti-MM agent, dexamethasone. Our data showed that SRT1720 remarkably enhances the anti-MM activity of both bortezomib and dexamethasone.

Collectively, our preclinical studies demonstrate potent *in vitro* and *in vivo* anti-MM activity of SRT1720. These findings provide the framework for clinical trials of SRT1720, alone or in combination with bortezomib or dexamethasone, to increase response, overcome drug resistance, reduce side effects, and improve patient outcome in MM.

Acknowledgments

Grant support: This investigation was supported by National Institutes of Health grants SPORE-P50100707, PO1-CA078378, and RO1CA050947. KCA is an ACS Clinical Research Professor.

References

Abdelmohsen K, Pullmann R Jr, Lal A, Kim HH, Galban S, Yang X, Blethrow JD, Walker M, Shubert J, Gillespie DA, Furneaux H, Gorospe M. Phosphorylation of HuR by Chk2 regulates SIRT1 expression. Mol Cell. 2007; 25:543–557. [PubMed: 17317627]

Avet-Loiseau H, Attal M, Moreau P, Charbonnel C, Garban F, Hulin C, Leyvraz S, Michallet M, Yakoub-Agha I, Garderet L, Marit G, Michaux L, Voillat L, Renaud M, Grosbois B, Guillerm G, Benboubker L, Monconduit M, Thieblemont C, Casassus P, Caillot D, Stoppa AM, Sotto JJ, Wetterwald M, Dumontet C, Fuzibet JG, Azais I, Dorvaux V, Zandecki M, Bataille R, Minvielle S, Harousseau JL, Facon T, Mathiot C. Genetic abnormalities and survival in multiple myeloma: the experience of the Intergroupe Francophone du Myelome. Blood. 2007; 109:3489–3495. [PubMed: 17209057]

Bergsagel PL, Kuehl WM. Molecular pathogenesis and a consequent classification of multiple myeloma. J Clin Oncol. 2005; 23:6333–6338. [PubMed: 16155016]

Bergsagel PL, Chesi M, Nardini E, Brents LA, Kirby SL, Kuehl WM. Promiscuous translocations into immunoglobulin heavy chain switch regions in multiple myeloma. Proc Natl Acad Sci U S A. 1996; 93:13931–13936. [PubMed: 8943038]

Bhalla S, Balasubramanian S, David K, Sirisawad M, Buggy J, Mauro L, Prachand S, Miller R, Gordon LI, Evens AM. PCI-24781 induces caspase and reactive oxygen species-dependent apoptosis through NF-kappaB mechanisms and is synergistic with bortezomib in lymphoma cells. Clin Cancer Res. 2009; 15:3354–3365. [PubMed: 19417023]

Bhardwaj A, Sethi G, Vadhan-Raj S, Bueso-Ramos C, Takada Y, Gaur U, Nair AS, Shishodia S, Aggarwal BB. Resveratrol inhibits proliferation, induces apoptosis, and overcomes chemoresistance through down-regulation of STAT3 and nuclear factor-kappaB-regulated antiapoptotic and cell survival gene products in human multiple myeloma cells. Blood. 2007; 109:2293–2302. [PubMed: 17164350]

Borra MT, O'Neill FJ, Jackson MD, Marshall B, Verdin E, Foltz KR, Denu JM. Conserved enzymatic production and biological effect of O-acetyl-ADP-ribose by silent information regulator 2-like NAD +-dependent deacetylases. J Biol Chem. 2002; 277:12632–12641. [PubMed: 11812793]

Bossy-Wetzel E, Green DR. Apoptosis: checkpoint at the mitochondrial frontier. Mutat Res. 1999; 434:243–251. [PubMed: 10486595]

Burger R, Guenther A, Bakker F, Schmalzing M, Bernand S, Baum W, Duerr B, Hocke GM, Steininger H, Gebhart E, Gramatzki M. Gp130 and ras mediated signaling in human plasma cell line INA-6: a cytokine-regulated tumor model for plasmacytoma. Hematol J. 2001; 2:42–53. [PubMed: 11920233]

Catley L, Weisberg E, Kiziltepe T, Tai YT, Hideshima T, Neri P, Tassone P, Atadja P, Chauhan D, Munshi NC, Anderson KC. Aggresome induction by proteasome inhibitor bortezomib and {alpha}-tubulin hyperacetylation by tubulin deacetylase (TDAC) inhibitor LBH589 are synergistic in myeloma cells. Blood. 2006; 108:3441–3449. [PubMed: 16728695]

Chauhan D, Uchiyama H, Akbarali Y, Urashima M, Yamamoto K, Libermann TA, Anderson KC. Multiple myeloma cell adhesion-induced interleukin-6 expression in bone marrow stromal cells involves activation of NF-kappa B. Blood. 1996; 87:1104–1112. [PubMed: 8562936]

Chauhan D, Singh A, Brahmandam M, Podar K, Hideshima T, Richardson P, Munshi N, Palladino MA, Anderson KC. Combination of proteasome inhibitors bortezomib and NPI-0052 trigger in vivo synergistic cytotoxicity in multiple myeloma. Blood. 2008; 111:1654–1664. [PubMed: 18006697]

Chauhan D, Singh AV, Ciccarelli B, Richardson PG, Palladino MA, Anderson KC. Combination of novel proteasome inhibitor NPI-0052 and lenalidomide trigger in vitro and in vivo synergistic cytotoxicity in multiple myeloma. Blood. 2010; 115:834–845. [PubMed: 19965674]

Chen D, Pacal M, Wenzel P, Knoepfler PS, Leone G, Bremner R. Division and apoptosis of E2f-deficient retinal progenitors. Nature. 2009; 462:925–929. [PubMed: 20016601]

Chua KF, Mostoslavsky R, Lombard DB, Pang WW, Saito S, Franco S, Kaushal D, Cheng HL, Fischer MR, Stokes N, Murphy MM, Appella E, Alt FW. Mammalian SIRT1 limits replicative life span in response to chronic genotoxic stress. Cell Metab. 2005; 2:67–76. [PubMed: 16054100]

Dai H, Kustigian L, Carney D, Case A, Considine T, Hubbard BP, Perni RB, Riera TV, Szczepankiewicz B, Vlasuk GP, Stein RL. SIRT1 activation by small molecules: kinetic and biophysical evidence for direct interaction of enzyme and activator. J Biol Chem. 2010; 285:32695–32703. [PubMed: 20702418]

Dai Y, Chen S, Kramer LB, Funk VL, Dent P, Grant S. Interactions between bortezomib and romidepsin and belinostat in chronic lymphocytic leukemia cells. Clin Cancer Res. 2008; 14:549–558. [PubMed: 18223231]

Dasmahapatra G, Lembersky D, Kramer L, Fisher R, Friedberg J, Dent P, Grant S. The pan-HDAC inhibitor vorinostat potentiates the activity of the proteasome inhibitor carfilzomib in human DLBCL cells in vitro and in vivo. Blood. 2010; 115:4478–4487. [PubMed: 20233973]

Davies FE, Dring AM, Li C, Rawstron AC, Shammas MA, O'Connor SM, Fenton JA, Hideshima T, Chauhan D, Tai IT, Robinson E, Auclair D, Rees K, Gonzalez D, Ashcroft AJ, Dasgupta R, Mitsiades C, Mitsiades N, Chen LB, Wong WH, Munshi NC, Morgan GJ, Anderson KC. Insights into the multistep transformation of MGUS to myeloma using microarray expression analysis. Blood. 2003; 102:4504–4511. [PubMed: 12947006]

Firestein R, Blander G, Michan S, Oberdoerffer P, Ogino S, Campbell J, Bhimavarapu A, Luikenhuis S, de Cabo R, Fuchs C, Hahn WC, Guarente LP, Sinclair DA. The SIRT1 deacetylase suppresses intestinal tumorigenesis and colon cancer growth. PLoS One. 2008; 3:e2020. [PubMed: 18414679]

Ford J, Jiang M, Milner J. Cancer-specific functions of SIRT1 enable human epithelial cancer cell growth and survival. Cancer Res. 2005; 65:10457–10463. [PubMed: 16288037]

Fu M, Liu M, Sauve AA, Jiao X, Zhang X, Wu X, Powell MJ, Yang T, Gu W, Avantaggiati ML, Pattabiraman N, Pestell TG, Wang F, Quong AA, Wang C, Pestell RG. Hormonal control of androgen receptor function through SIRT1. Mol Cell Biol. 2006; 26:8122–8135. [PubMed: 16923962]

Funk JA, Odejinmi S, Schnellmann RG. SRT1720 induces mitochondrial biogenesis and rescues mitochondrial function after oxidant injury in renal proximal tubule cells. J Pharmacol Exp Ther. 2010; 333:593–601. [PubMed: 20103585]

Grant S, Easley C, Kirkpatrick P. Vorinostat. Nat Rev Drug Discov. 2007; 6:21–22. [PubMed: 17269160]

Greenstein S, Krett NL, Kurosawa Y, Ma C, Chauhan D, Hideshima T, Anderson KC, Rosen ST. Characterization of the MM.1 human multiple myeloma (MM) cell lines. A model system to elucidate the characteristics, behavior, and signaling of steroid-sensitive and -resistant MM cells. Exp Hematol. 2003; 31:271–282. [PubMed: 12691914]

Harper CE, Patel BB, Wang J, Arabshahi A, Eltoum IA, Lamartiniere CA. Resveratrol suppresses prostate cancer progression in transgenic mice. Carcinogenesis. 2007; 28:1946–1953. [PubMed: 17675339]

Haigis MC, Sinclair DA. Mammalian sirtuins: biological insights and disease relevance. Annu Rev Pathol. 2010; 5:253–295. [PubMed: 20078221]

Heltweg B, Gatbonton T, Schuler AD, Posakony J, Li H, Goehle S, Kollipara R, Depinho RA, Gu Y, Simon JA, Bedalov A. Antitumor activity of a small-molecule inhibitor of human silent information regulator 2 enzymes. Cancer Res. 2006; 66:4368–4377. [PubMed: 16618762]

Hideshima T, Chauhan D, Shima Y, Raje N, Davies FE, Tai YT, Treon SP, Lin B, Schlossman RL, Richardson P, Muller G, Stirling DI, Anderson KC. Thalidomide and its analogs overcome drug resistance of human multiple myeloma cells to conventional therapy. Blood. 2000; 96:2943–2950. [PubMed: 11049970]

Hideshima T, Chauhan D, Richardson P, Mitsiades C, Mitsiades N, Hayashi T, Munshi N, Dang L, Castro A, Palombella V, Adams J, Anderson KC. NF-kappa B as a therapeutic target in multiple myeloma. J Biol Chem. 2002; 277:16639–16647. [PubMed: 11872748]

Hideshima T, Bradner JE, Wong J, Chauhan D, Richardson P, Schreiber SL, Anderson KC. Small-molecule inhibition of proteasome and aggresome function induces synergistic antitumor activity in multiple myeloma. Proc Natl Acad Sci U S A. 2005; 120:8567–8572. [PubMed: 15937109]

Hideshima T, Mitsiades C, Tonon G, Richardson PG, Anderson KC. Understanding multiple myeloma pathogenesis in the bone marrow to identify new therapeutic targets. Nat Rev Cancer. 2007; 7:585–598. [PubMed: 17646864]

Imai S, Armstrong CM, Kaeberlein M, Guarente L. Transcriptional silencing and longevity protein Sir2 is an NAD-dependent histone deacetylase. Nature. 2000; 403:795–800. [PubMed: 10693811]

Jackson MD, Denu JM. Structural identification of 2′- and 3′-O-acetyl-ADP-ribose as novel metabolites derived from the Sir2 family of beta -NAD+-dependent histone/protein deacetylases. J Biol Chem. 2002; 277:18535–18544. [PubMed: 11893743]

Kabra N, Li Z, Chen L, Li B, Zhang X, Wang C, Yeatman T, Coppola D, Chen J. SirT1 is an inhibitor of proliferation and tumor formation in colon cancer. J Biol Chem. 2009; 284:18210–18217. [PubMed: 19433578]

Kamel C, Abrol M, Jardine K, He X, McBurney MW. SirT1 fails to affect p53-mediated biological functions. Aging Cell. 2006; 5:81–88. [PubMed: 16441846]

Kumar S, Witzig TE, Timm M, Haug J, Wellik L, Fonseca R, Greipp PR, Rajkumar SV. Expression of VEGF and its receptors by myeloma cells. Leukemia. 2003; 17:2025–2031. [PubMed: 14513053]

Lazebnik YA, Kaufmann SH, Desnoyers S, Poirier GG, Earnshaw WC. Cleavage of poly (ADP-ribose) polymerase by a proteinase with properties like ICE. Nature. 1994; 371:346–347. [PubMed: 8090205]

LeBlanc R, Catley LP, Hideshima T, Lentzsch S, Mitsiades CS, Mitsiades N, Neuberg D, Goloubeva O, Pien CS, Adams J, Gupta D, Richardson PG, Munshi NC, Anderson KC. Proteasome inhibitor

PS-341 inhibits human myeloma cell growth in vivo and prolongs survival in a murine model. Cancer Res. 2002; 62:4996–5000. [PubMed: 12208752]

Miller LK. An exegesis of IAPs: salvation and surprises from BIR motifs. Trends Cell Biol. 1999; 9:323–328. [PubMed: 10407412]

Milne JC, Denu JM. The Sirtuin family: therapeutic targets to treat diseases of aging. Curr Opin Chem Biol. 2008; 12:11–17. [PubMed: 18282481]

Narala SR, Allsopp RC, Wells TB, Zhang G, Prasad P, Coussens MJ, Rossi DJ, Weissman IL, Vaziri H. SIRT1 acts as a nutrient-sensitive growth suppressor and its loss is associated with increased AMPK and telomerase activity. Mol Biol Cell. 2008; 19:1210–1219. [PubMed: 18184747]

Ota H, Tokunaga E, Chang K, Hikasa M, Iijima K, Eto M, Kozaki K, Akishita M, Ouchi Y, Kaneki M. Sirt1 inhibitor, Sirtinol, induces senescence-like growth arrest with attenuated Ras-MAPK signaling in human cancer cells. Oncogene. 2006; 25:176–185. [PubMed: 16170353]

Pacholec M, Bleasdale JE, Chrunyk B, Cunningham D, Flynn D, Garofalo RS, Griffith D, Griffor M, Loulakis P, Pabst B, Qiu X, Stockman B, Thanabal V, Varghese A, Ward J, Withka J, Ahn K. SRT1720, SRT2183, SRT1460, and resveratrol are not direct activators of SIRT1. J Biol Chem. 2010; 285:8340–8351. [PubMed: 20061378]

Podar K, Tai YT, Davies FE, Lentzsch S, Sattler M, Hideshima T, Lin BK, Gupta D, Shima Y, Chauhan D, Mitsiades C, Raje N, Richardson P, Anderson KC. Vascular endothelial growth factor triggers signaling cascades mediating multiple myeloma cell growth and migration. Blood. 2001; 98:428–435. [PubMed: 11435313]

Podar K, Tai YT, Lin BK, Narsimhan RP, Sattler M, Kijima T, Salgia R, Gupta D, Chauhan D, Anderson KC. Vascular Endothelial Growth Factor-induced Migration of Multiple Myeloma Cells Is Associated with beta 1 Integrin- and Phosphatidylinositol 3-Kinase-dependent PKCalpha Activation. J Biol Chem. 2002; 277:7875–7881. [PubMed: 11751905]

Rajkumar SV, Witzig TE. A review of angiogenesis and antiangiogenic therapy with thalidomide in multiple myeloma. Cancer Treat Rev. 2000; 26:351–362. [PubMed: 11006136]

Sauve AA. Pharmaceutical strategies for activating sirtuins. Curr Pharm Des. 2009; 15:45–56. [PubMed: 19149602]

Sexton E, Van Themsche C, LeBlanc K, Parent S, Lemoine P, Asselin E. Resveratrol interferes with AKT activity and triggers apoptosis in human uterine cancer cells. Mol Cancer. 2006; 5:45. [PubMed: 17044934]

Solomon JM, Pasupuleti R, Xu L, McDonagh T, Curtis R, DiStefano PS, Huber LJ. Inhibition of SIRT1 catalytic activity increases p53 acetylation but does not alter cell survival following DNA damage. Mol Cell Biol. 2006; 26:28–38. [PubMed: 16354677]

Strasser A, O'Connor L, Dixit VM. Apoptosis signaling. Annu Rev Biochem. 2000; 69:217–245. [PubMed: 10966458]

Stunkel W, Peh BK, Tan YC, Nayagam VM, Wang X, Salto-Tellez M, Ni B, Entzeroth M, Wood J. Function of the SIRT1 protein deacetylase in cancer. Biotechnol J. 2007; 2:1360–1368. [PubMed: 17806102]

Vacca A, Ribatti D, Presta M, Minischetti M, Iurlaro M, Ria R, Albini A, Bussolino F, Dammacco F. Bone marrow neovascularization, plasma cell angiogenic potential, and matrix metalloproteinase-2 secretion parallel progression of human multiple myeloma. Blood. 1999; 93:3064–3073. [PubMed: 10216103]

Wang RH, Sengupta K, Li C, Kim HS, Cao L, Xiao C, Kim S, Xu X, Zheng Y, Chilton B, Jia R, Zheng ZM, Appella E, Wang XW, Ried T, Deng CX. Impaired DNA damage response, genome instability, and tumorigenesis in SIRT1 mutant mice. Cancer Cell. 2008; 14:312–323. [PubMed: 18835033]

Yeung F, Hoberg JE, Ramsey CS, Keller MD, Jones DR, Frye RA, Mayo MW. Modulation of NF-kappaB-dependent transcription and cell survival by the SIRT1 deacetylase. EMBO J. 2004; 23:2369–2380. [PubMed: 15152190]

Yoshizaki T, Milne JC, Imamura T, Schenk S, Sonoda N, Babendure JL, Lu JC, Smith JJ, Jirousek MR, Olefsky JM. SIRT1 exerts anti-inflammatory effects and improves insulin sensitivity in adipocytes. Mol Cell Biol. 2009; 29:1363–1374. [PubMed: 19103747]

Yuan Z, Seto E. A functional link between SIRT1 deacetylase and NBS1 in DNA damage response. Cell Cycle. 2007; 6:2869–2871. [PubMed: 18156798]

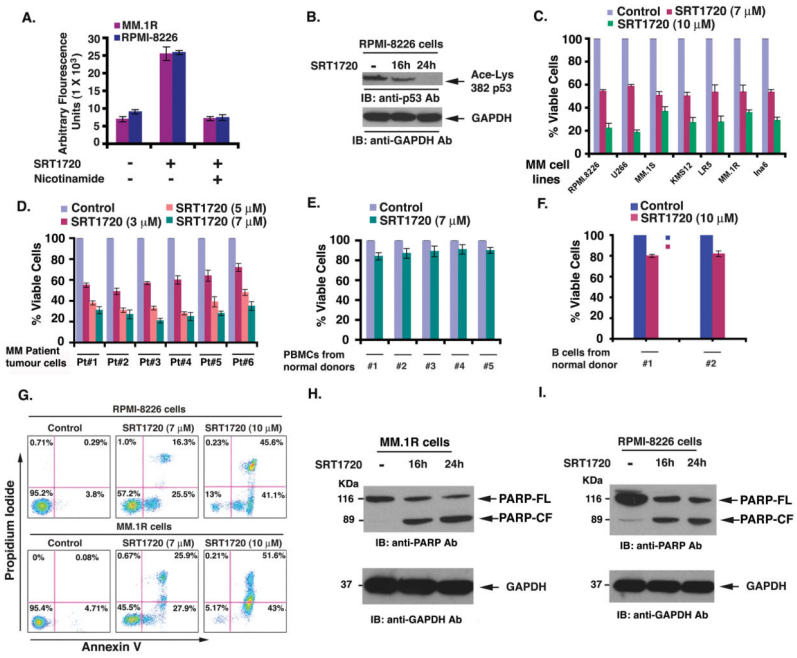

Figure 1. SIRT1720 induces SIRT1 enzyme activity *in vitro* and triggers MM cell death

(A) MM.1R and RPMI-8226 cells were treated with SRT1720 (7 μM) in the presence or absence of SIRT1 inhibitor nicotinamide for 6 h and harvested; extracts were then analysed for SIRT1 enzyme activity. (B) RPMI-8226 cells were treated with SRT1720 (7 μM) and harvested; protein lysates were subjected to immunoblot (IB) analysis with antibodies (Ab) specifically against acetylated p53 and GAPDH. Blots shown are representative of 3 independent experiments. (C) MM cell lines were treated with or without SIRT1720 at the indicated concentrations for 24h, followed by assessment for cell viability using MTT assays. Raw data from MTT assays were normalized to the percentage of viable cells in control (as 100%) versus drug-treated cells. Data presented are means ± standard deviation (SD) (n =3; $P < 0.005$ for all cell lines). (D) Purified patient MM cells (CD138-positive) were treated with SIRT1720 at the indicated concentrations for 24 h, and cell viability was measured. Raw data were normalized to the percentage of viable cells in control (as 100%) versus drug-treated cells. SRT1720 triggered specific reduction in the percentage of the viable primary MM cells versus untreated (control) cells. Values represent means of triplicate cultures ± SD ($P < 0.05$ for all patient samples). (E) PBMCs from healthy donors were treated with indicated concentrations of SIRT1720, and then analysed for viability using the MTT assay. Raw data from MTT assays were normalized to the percentage of viable cells in control (as 100%) versus drug-treated cells. Data presented are means ± SD (n =2; $P < 0.05$). (F) Normal B cells were treated with indicated concentrations of SIRT1720, and then analysed for viability using the MTT assay. Data presented are means ± SD (n =2; $P < 0.05$) (G) RPMI-8226 and MM.1R cell lines were treated with SRT1720 for 24 h, and then analysed for apoptosis using Annexin V/PI staining assay. (H and I) MM.1R and RPMI-8226 cells were treated with SRT1720 (7 μM) and harvested; whole cell lysates were subjected to immunoblot analysis with anti-PARP, or anti-GAPDH Abs. FL, full length; CF, cleaved fragment. Blots shown are representative of 3 independent experiments.

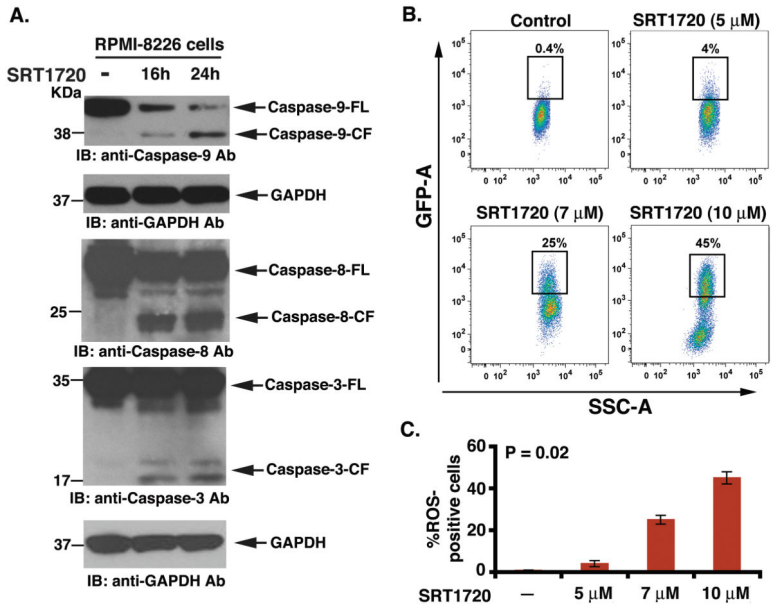

Figure 2. SRT1720 triggers activation of both intrinsic (caspase-8) and extrinsic (caspase-9) apoptotic signalling

(A) RPMI-8226 cells were treated with SRT1720 (7 μM) for the indicated times and harvested. Total proteins were subjected to immunoblot analysis (IB) with anti-caspase-9, caspase-8, caspase-3, or GAPDH Abs. FL, full length; CF, cleaved fragment. Blots shown are representative of three independent experiments. (B) RPMI-8226 cells were treated with SRT1720 at the indicated concentrations for 6 h, harvested, stained with the membrane permeable dye dihydroethidium for the last 15 min, and analysed by flow cytometry. Results are mean ± SD of three independent experiments ($n = 3$; $P < 0.005$). (C) Bar graph represents quantification of the percentage of reactive oxygen species (ROS)-positive cells from the experiment in panel 'B'.

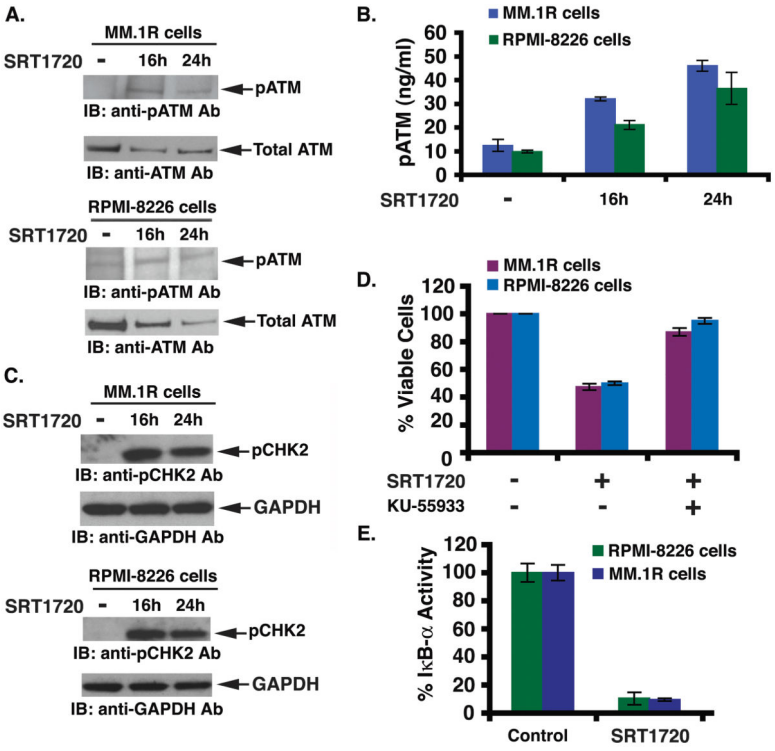

Figure 3. SRT1720-induced apoptosis is associated with activation of ATM/CHK2 and downregulation of the NF-κB signalling pathway

(A) MM.1R and RPMI-8226 cells were treated with SRT1720 (7 μM) and harvested; total proteins were subjected to immunoblot analysis with anti-phosphorylated ATM (anti-pATM) or anti-ATM Abs. Blots shown are representative of three independent experiments. (B) MM.1R and RPMI-8226 cells were treated with SRT1720 (7 μM) and harvested; extracts were subjected to ELISA ($P < 0.005$; $n = 3$). (C) MM.1R and RPMI-8226 cells were treated with SRT1720 (7 μM) and harvested; total proteins were subjected to immunoblot analysis with anti-phosphorylated CHK2 (anti-pCHK2) or anti-CHK2 Abs. Blots shown are representative of three independent experiments. (D) MM.1R and RPMI-8226 cells were treated with SIRT1720 in the presence or absence of the ATM inhibitor KU55933 for 24 h, followed by assessment for cell viability using MTT assays. Data presented are means ± SD ($n = 3$; $P < 0.05$). (E) MM.1R and RPMI-8226 cells were treated with SIRT1720 (7 μM) for 24 h, and extracts were then analysed for NF-κB activity by measuring phosphorylated IκB-α using both ELISA kits. Data presented are means ± SD ($n = 3$; $P < 0.05$).

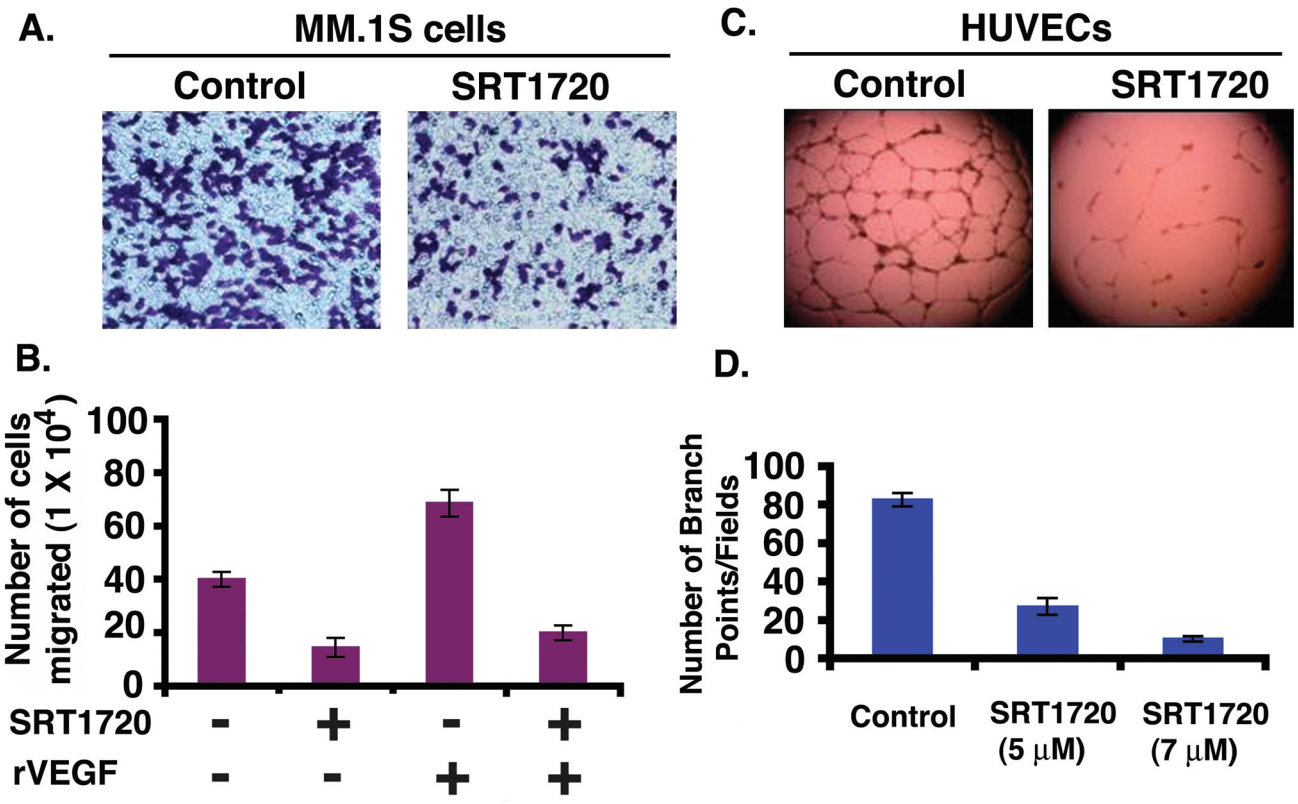

Figure 4. SRT1720 blocks migration and inhibits *in vitro* capillary tubule formation

(A) MM.1S cells were pretreated with 5 μM SRT1720 for 12h; cells (>90% viable) were then washed and cultured in serum-free medium. After a 2-h incubation, cells (viability > 90%) were plated on a fibronectin-coated polycarbonate membrane in the upper chamber of Transwell inserts, and exposed to serum-containing medium in the lower chamber for 4 h. Cells migrating to the bottom face of the membrane were fixed with 90% ethanol and stained with crystal violet (magnification: 10X/0.25 NA oil). A total of 3 randomly selected fields were examined for cells that had migrated from top to bottom chambers. The images arerepresentative of 3 experiments with similar results. (B) Cells were plated as in 'A' and the effect of SRT1720 on migration was assessed in the presence or absence of recombinant vascular endothelial growth factor (rVEGF). The bar graph represents quantification of migrated cells. Data presented are means ± SD (n = 3; P = 0.04 for control *versus* SRT1720-treated cells). Error bars represent SD. (C) HUVECs were cultured in the presence or absence of SRT1720 for 12 h, and then assessed for *in vitro* angiogenesis using Matrigel capillary-like tube structure formation assays (magnification: 4X/0.10 NA oil, media: EBM-2). is the images are representative of 3 experiments with similar results. *In vitro* angiogenesis is evidenced by capillary tube branch formation (dark brown). Data represents means ± SD (n=3; P < 0.05). (D) The bar graph represents quantification of capillary-like tube structure formation by vehicle alone and SRT1720-treated cells. Branch points in several random view fields/well were counted, values were averaged and statistically significant differences were measured using Student's *t*-test. Data presented are means ± SD

(n = 3; P = 0.02 for control *versus* SRT1720-treated cells). Error bars represent standard deviation (SD).

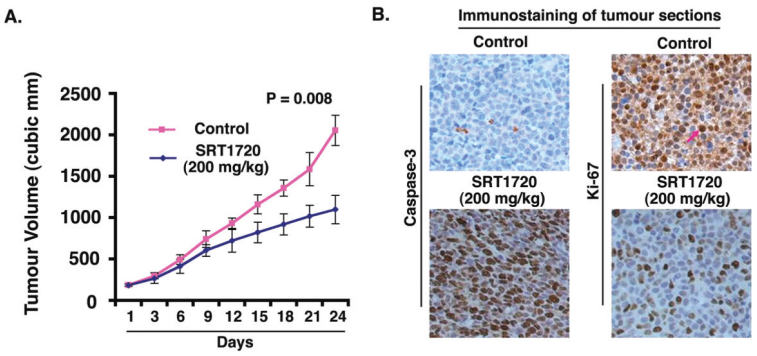

Figure 5. SRT1720 inhibits growth of xenografted human MM cells in mice

(A) MM.1S cells alone (6×10^6 cells/mouse) were implanted in the rear flank of female BNX mice (5–7 weeks of age at the time of tumour challenge). On Day 27–30, mice were randomized to treatment groups and treated intravenously with vehicle or SRT1720 (200 mg/kg). Mice were treated for two consecutive days, repeated weekly for 7 weeks. Data are presented as mean tumour volume ± standard error of the mean (SEM) (n = 6 group; P = 0.008). A representative experiment is shown. (B) Tumours were removed from control untreated or SRT1720-treated mice, followed by immunohistochemical analysis with antibodies against Caspase-3, and Ki-67. Scale bar, 10 μM. Dark brown: marker-positive cells in all cases. Micrographs are representative of tumour sections from two different mice in each group.

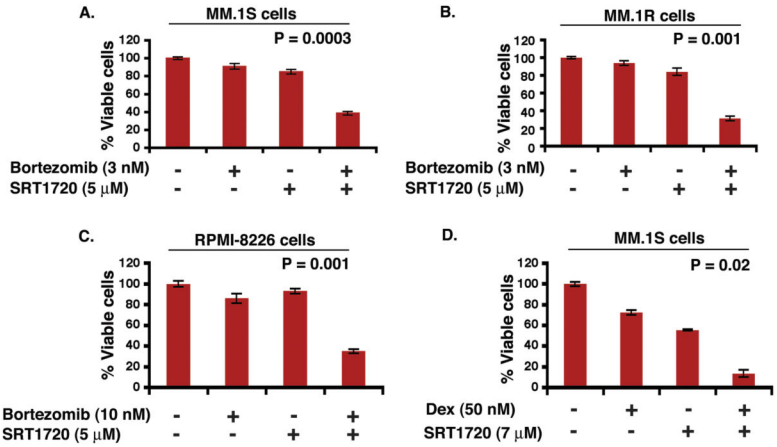

Figure 6. Combination of low doses of SRT1720 and bortezomib or dexamethasone enhances MM cell death

Low doses of SRT1720 and bortezomib trigger additive anti-MM activity in MM cells. MM.1S (A), MM.1R (B), or RPMI-8226 (C) cells were treated for 24 h with the indicated concentrations of SRT1720, bortezomib, or SRT1720 plus bortezomib; and then assessed for viability using MTT assays (mean ± SD; n = 3). (D) Low doses of SRT1720 and dexamethasone trigger additive anti-MM activity in MM cells. MM.1S cells were treated for 24 h with indicated concentrations of SRT1720, dexamethasone, or SRT1720 plus dexamethasone and then assessed for viability using MTT assays. Shown is mean ± SD of three independent experiments.